PAPER • OPEN ACCESS

Analysis of principles of equivalence and suppression in resistivity sounding technique

To cite this article: Oluseun Adetola Sanuade *et al* 2019 *J. Phys.: Conf. Ser.* **1299** 012065

View the article online for updates and enhancements.

Analysis of principles of equivalence and suppression in resistivity sounding technique

Oluseun Adetola SANUADE[1]*, Joel Olayide AMOSUN[2], KehindeDavid OYEYEMI[3], Abayomi Adesola OLAOJO[4], Tokunbo Sanmi FAGBEMIGUN[2] Jane Idowu FALOYO[5]

[1]Geosciences Department, King Fahd University of Petroleum & Minerals, Dhahran, Saudi Arabia.
[2]Department of Geophysics, Federal University Oye-Ekiti, Ekiti State, Nigeria
[3]Department of Industrial Physics, Covenant University, Ota, Ogun State, Nigeria
[4]Department of Earth Sciences, Ajayi Crowther University, Oyo, Oyo State, Nigeria.
[5]Department of Applied Geophysics, Federal University of Technology Akure, Nigeria.

*sheunsky@gmail.com

Abstract. The principles of equivalence and suppression in resistivity sounding technique are phenomena where different resistivity models may produce resistivity curves that are essentially the same. The understanding of these phenomena could be of great importance in using resistivity sounding technique for citing boreholes in places underlain by Basement Complex rocks. In such areas, it would be difficult to identify the fractured/weathered bedrock from the sounding interpretation. This is because the resistivity of the weathered layer is usually intermediate between those of the adjacent layers (i.e. residual overburden) on top and the fresh bedrock below. Therefore, it is important to analyse the problems of suppression and equivalence in resistivity sounding data for estimating thickness and resistivity of the subsurface layers. Several resistivity models were generated ranging from two-layer to five-layer models to investigate these phenomena. The apparent resistivity curves were plotted for these models. The results show that the problems of suppression and equivalence exist in resistivity sounding data. Hence, geophysicists should not make any a priori quantitative inferences using the shape of the resistivity sounding curve.

Keywords: Equivalence, suppression, resistivity, models.

1. Introduction

The principle of equivalence in resistivity sounding is a phenomenon where different combinations of resistivity values and the thicknesses of the subsurface layer produce the same/similar apparent resistivity curves [1]. This is a well-known problem in the interpretation of sounding data which could occur 1D, 2D or 3D geoelectrical sounding data. This problem has been studied in many 1D interpretations of geoelectrical sounding data [2-11]. The principle of equivalence is such that several models produce the same results which often lead to ambiguity in Physics of 1D interpretations because several layered models basically produce same or similar response [9-11]. For instance, if there are layers that are conductive in between two resistive layers, in which lateral

conductance (σ_h) is the same, this will lead to equivalence. Also, equivalence would occur in a situation where a resistive layer is between two conductive layers, in which they have the same transverse resistance (ρ_h).

Moreover, the suppression principle is an essential principle which needs to be clearly understood to properly evaluate the interpretations of resistivity sounding curves. This principle states that, a thin layer with resistivity values that lies between the overlying and underlying resistivity values would produce no effect on the resistivity curves [7, 10-12]; thereby such thin layers would be missed during resistivity sounding data interpretation. In practical terms, if a thick section of shale overlies a thin freshwater-saturated sandstone and the sandstone is underlain by the basement complex, a resistivity sounding data in the subsurface would produce resistivity curve in which the thin layer of sandstone would not have effect on the shape of the curve and hence would not be detected by the resistivity method. The principle of suppression is an essential problems of resistivity soundings for the detection of successive groundwater aquifers [7] and needs to be studied. Therefore, an inversion solution in resistivity sounding data may not produce the geological reality [13] and would lead to the non-uniqueness of the resistivity data interpretation [7].

More so, these principles could lead to error when the depth to the fresh basement is to be determined [14]. The phenomena are also very important during the selection of borehole sites in areas that are underlain by crystalline basement complex rocks. In such areas, identifying the fractured or weathered zones from the sounding interpretation is often difficult [15]. This is because the resistivity of the fractured zone is always intermediate between the resistivity values of the adjacent layers (i.e. residual overburden). In this case, the fractured zone would not be identified on a resistivity sounding curve which may partly be the reason for variations in the depth to fresh basement estimated by resistivity sounding data and that confirmed by borehole drilling [16].

Therefore, objective of this study is to analyse the principles of suppression and equivalence in resistivity sounding data for estimating thickness and resistivity of the subsurface layers.

2. Methodology

In this study, the principles of equivalence and suppression were analysed using the workflow in Fig. 1.

```
┌──────────────────────────────────┐
│   1. Build a three-layer model   │
└──────────────────────────────────┘
                 │
      ┌──────────────────────────┐
      │  2. Plot resistivity curve │
      └──────────────────────────┘
                 │
      ┌──────────────────────────┐
      │   3. Remove middle layer  │
      └──────────────────────────┘
                 │
      ┌──────────────────────────┐
      │  4. Plot resistivity curve │
      └──────────────────────────┘
                 │
 ┌─────────────────────────────────────────┐
 │ 5. Select a new three-layer model by     │
 │ changing the thickness and resistivity   │
 │ of middle layer                          │
 └─────────────────────────────────────────┘
                 │
      ┌──────────────────────────┐
      │  6. Plot resistivity curve │
      └──────────────────────────┘
                 │
 ┌─────────────────────────────────────────┐
 │ 7. Select a new three-layer model with   │
 │ reduction of thickness of middle layer   │
 │ by a factor                              │
 └─────────────────────────────────────────┘
                 │
      ┌──────────────────────────┐
      │  8. Plot resistivity curve │
      └──────────────────────────┘
                 │
 ┌─────────────────────────────────────────────────┐
 │ 9. Select a new three-layer model with reduction │
 │ in resistivity contrast between the middle layer │
 │ and the overlying/underlying layer               │
 └─────────────────────────────────────────────────┘
                 │
      ┌──────────────────────────┐
      │  10. Plot resistivity curves │
      └──────────────────────────┘
                 │
 ┌─────────────────────────────────────────┐
 │ 11. Select a five-layer model with a     │
 │ thin middle layer of high resistivity    │
 └─────────────────────────────────────────┘
                 │
      ┌──────────────────────────┐
      │  12. Plot resistivity curve │
      └──────────────────────────┘
```
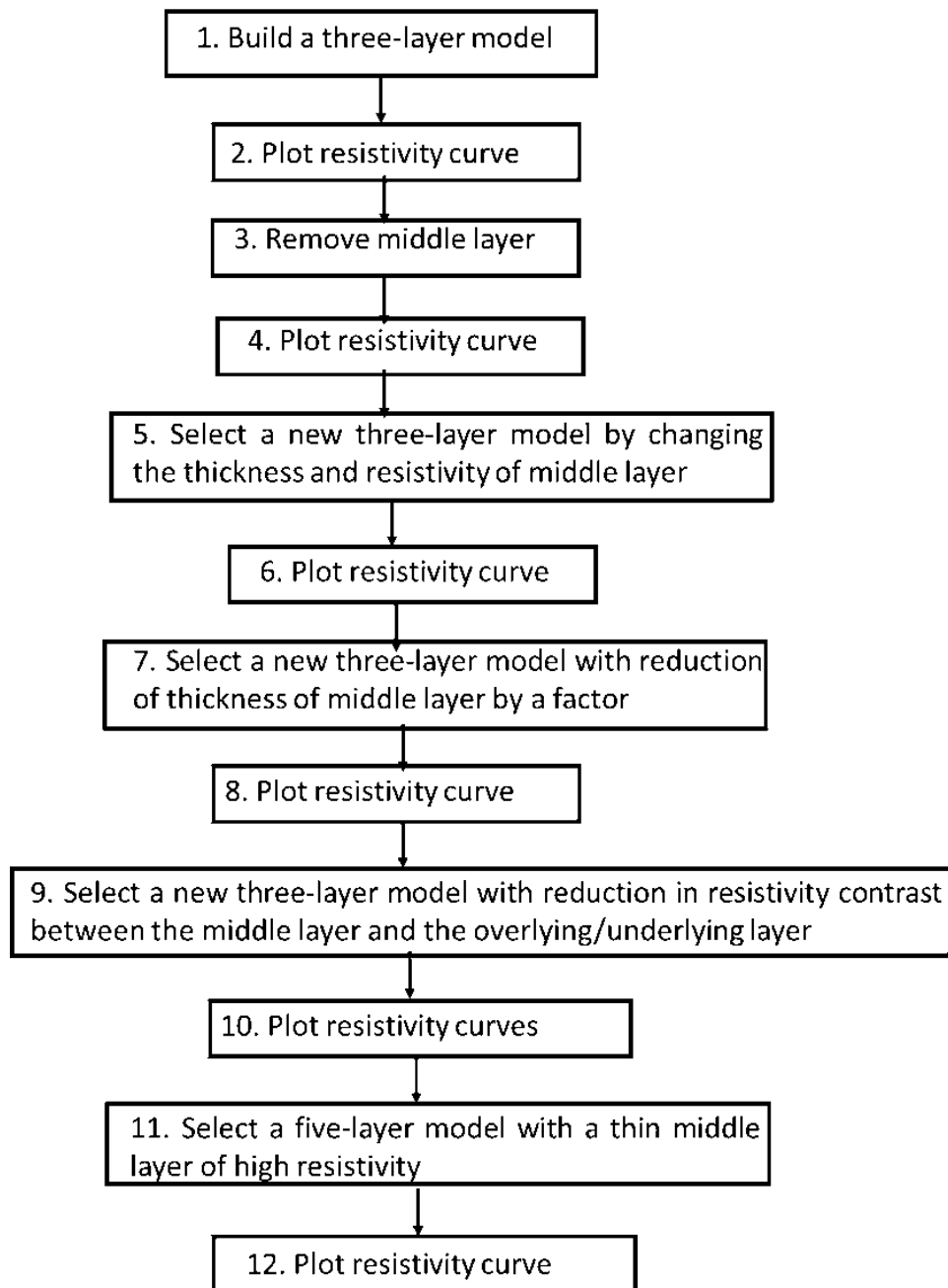
Fig. 1: Workflow for the analyses of principles of equivalence and suppression

The step-by-step explanation of the workflow is given below:

1. The analysis started by selecting a three-layer model, in which the middle layer is relatively conductive compared to the enclosing layers (Fig. 2).
2. The apparent resistivity sounding curve for the three-layer model is computed by convolution (Ghosh, 1971), using MATLAB 2018a for a Wenner array to generate curve. The theory involved in the computation of apparent resistivity is described in the next section.
3. We removed the middle layer from the three-layer model.
4. The resistivity sounding curve for the model in step 3 was also plotted to produceresistivity curve.

5.   A new three-layer model was selected with a different thickness and resistivity of middle layer.
6.   Resistivity sounding curve was generated for the model in step 5 to produce resistivity curve.
7.   A three-layer model was also selected with a reduced thickness of middle layer by a factor of 4 or more.
8.   The resistivity sounding curve for this model was then plotted to generate resistivity curve.
9.   A new three-layer model was selected with a reduction in the resistivity contrast between the middle layer and the overlying and underlying layer.
10.   The theoretical sounding curve for this model was plotted to produce resistivity curve.
11.   A five-layer model with a thin middle layer of high resistivity was generated.
12.   The resistivity sounding curve for the five-layer model was also plotted to generate resistivity curve.

2.1   Theory

The resistivity sounding curves for the models were computed by convolution [17] using MATLAB 2018a for a Wenner array.

For a 1D layered medium, the expression for the voltage from a point source of current on the Earth's surface (or the apparent resistivity (ρ_a) for a surface electrode configuration) could be written in the form of an infinite integral involving Bessel functions and a kernel function which are dependent on the layer resistivities and thicknesses. Therefore, the expression for ρ_a for the Wenner array is given by equation 1 [18].

$$\rho_a(A) = 2A \int_0^\infty T(\lambda)\{J_o(A\lambda) - J_o(2A\lambda)\}d\lambda \qquad\qquad 1$$

where A is the electrode spacing, J_o is the zero order Bessel function of the first kind, λ is a variable of integration with units of inverse distance and $T(\lambda)$ is the resistivity transform function, which is a function of the thicknesses of layer H_i and layer resistivities R_i. For a sequence of E-1 layers over a half-space R_E, the transform T_1 (transform of the entire section) was obtained by recursion using equation 2.

$$T_{j-i} = \frac{T_j + R_{j-i}\tanh(\lambda H_{j-i})}{1 + \frac{T_j \tanh(\lambda H_{j-i})}{R_{j-i}}} \quad j = E, E-1, \dots\dots 2 \qquad\qquad 2$$

with $T_E = R_E$

Equation 2 stacks layers together from the bottom layer (j=E) to the surface successively (j=2).

2.2   Convolution integral expression

The integrand in equation 1 is rapidly changing and the original method of evaluating the integral involved a series summation involving thousands of terms [19]. However, the integral can be cast in the form of convolution integrals and can be evaluated more efficiently by making substitutions; that is,

A = e^y; $\lambda = e^{-y}$; $d\lambda$ = $-e^{-y}dy$

Therefore, equation 1 can be transformed to equation 3.

$$\rho_a(x) = \int_{-\infty}^\infty T(y).h(x-y)dy \qquad\qquad 3$$

with:

$$h(u) = 2e^u\{J_o[e^u] - J_o[2e^u]\}4$$

where h(x-y) is the filter function or impulse response which was calculated through digital convolution using equation 5.

$$\rho_i = \sum T_j h_{i-j} = \sum T_{i-j} h_j \quad 5$$

h_j is the filter coefficients.

The present form of the solution of the integrals requires a different filter for the Wenner array. A single monopole filter function by Davis et al. [18] was used in this study. The filter is given by equation 6 and the monopole apparent resistivity is given by equation 7.

$$h(x - y) = J_o(e^{x-y})e^{x-y} \quad 6$$

$$\rho_m(x) = \int_{-\infty}^{\infty} T(y) . J_o(e^{x-y}) . e^{x-y} dy \qquad 7$$

The apparent resistivity for the Wenner array was computed in terms of the monopole resistivity using equation 8 [18].

$$\rho_a(x) = 2\rho_m(x) - \rho_m(x + log2) \quad 8$$

Davis et al. [18] derived a 34-point digital filter used in this study which relates values of monopole apparent resistivity to resistivity transform functions for the specific earth model by the convolution sum using equation 9.

$$\rho_i = \sum_{j=-22}^{11} T_{i-j} b_j \quad 9$$

Therefore, the transform function T*(y) for Wenner array is given by equation 10.

$$T^*(y) = 2T(y) - T(y + log2) \quad 10$$

where minimum and maximum values of y are given by equations 11 and 12.

$$y_{min} = y_{0-11} = -11\Delta x + 0.04634 \qquad\qquad 11$$
$$y_{max} = y_{12-(-22)} = 34\Delta x + 0.04634 \qquad\qquad 12$$

Therefore,

$$\rho_i(i\Delta x) = \sum_{j=-22}^{11} T^*[(i-j)\Delta x + 0.04634]b_j \qquad\qquad 13$$

3. Results and Discussion

The two layer resistivity model with layer thickness (H) = 10 m and layer resistivities of $R_1 = 10$ Ωm, $R_2 = 100$ Ωm is shown in Fig. 2. The apparent resistivity curve generated for this model is shown in Fig. 3.
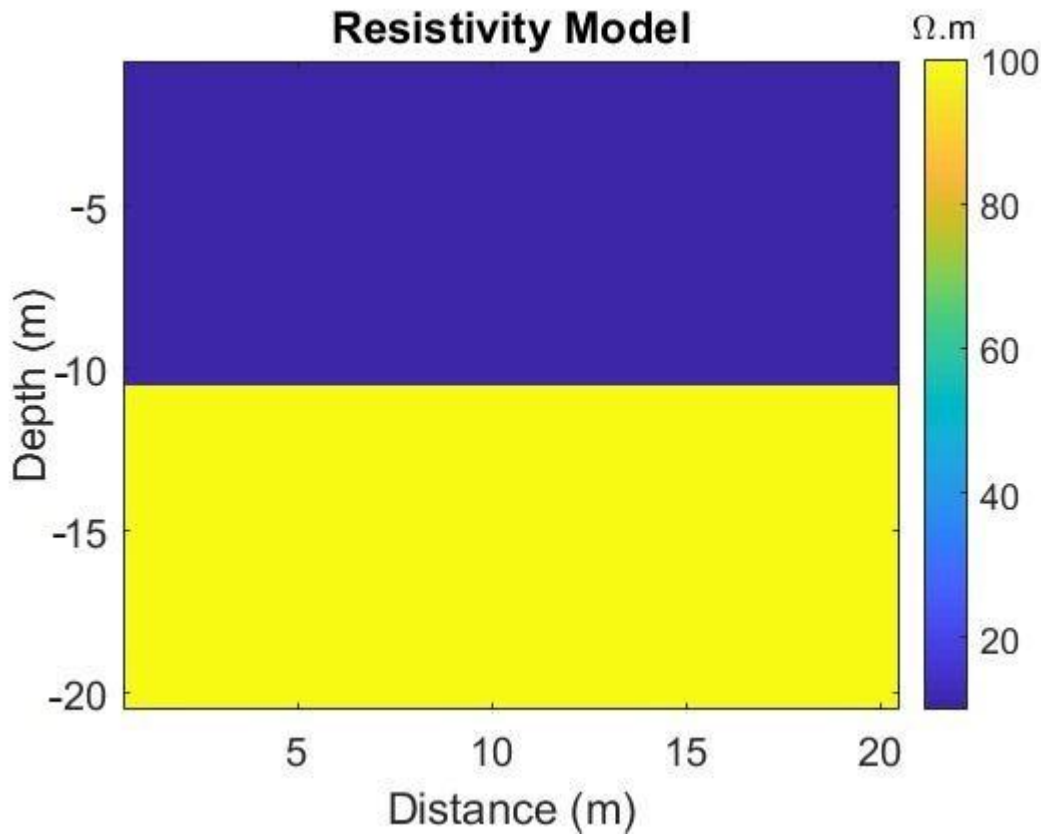
Fig. 2: A two-layer resistivity model. The upper layer resistivity is 10 Ωm, while the lower layer resistivity is 100 Ωm.
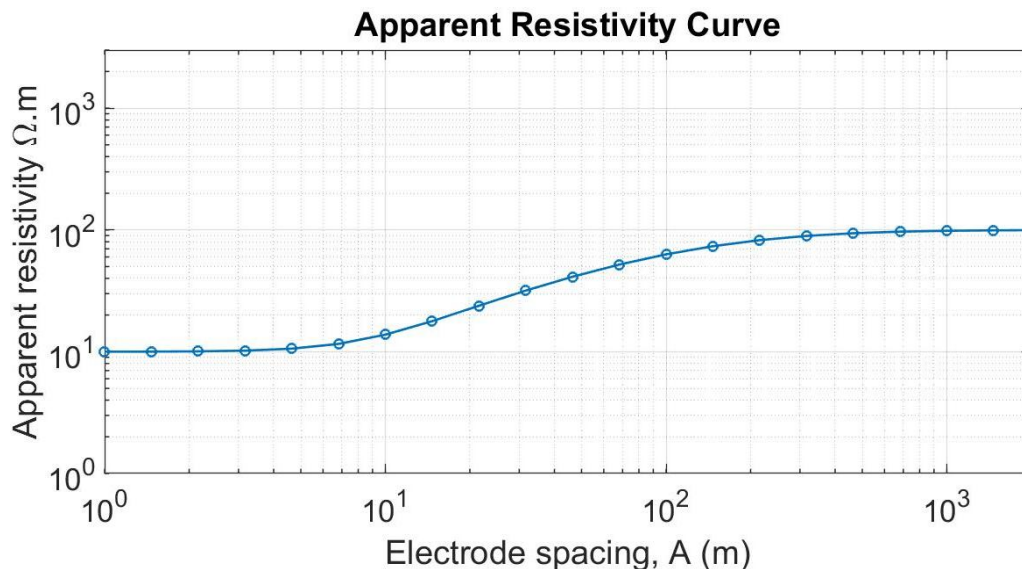

Fig. 3: Apparent resistivity curve for a two-layer model.

For the selected three-layer resistivity model (Fig. 4), the following parameters was used to generate the model:

$H_1 = 10\ m,\ H_2 = 15\ m,\ R_1 = 100\ \Omega m,\ R_2 = 20\ \Omega m,\ R_3 = 500\ \Omega m$

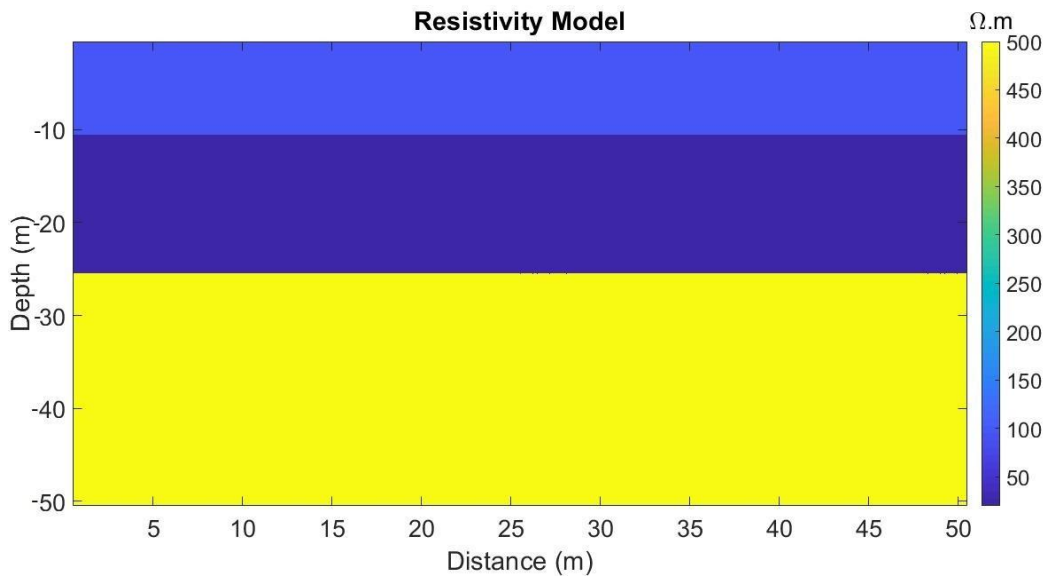In this model, the middle layer is relatively conductive compared to the enclosing layers (Fig. 4).

Figure 4: A three-layer resistivity model.

The apparent resistivity curve for this model is shown in Fig. 5.
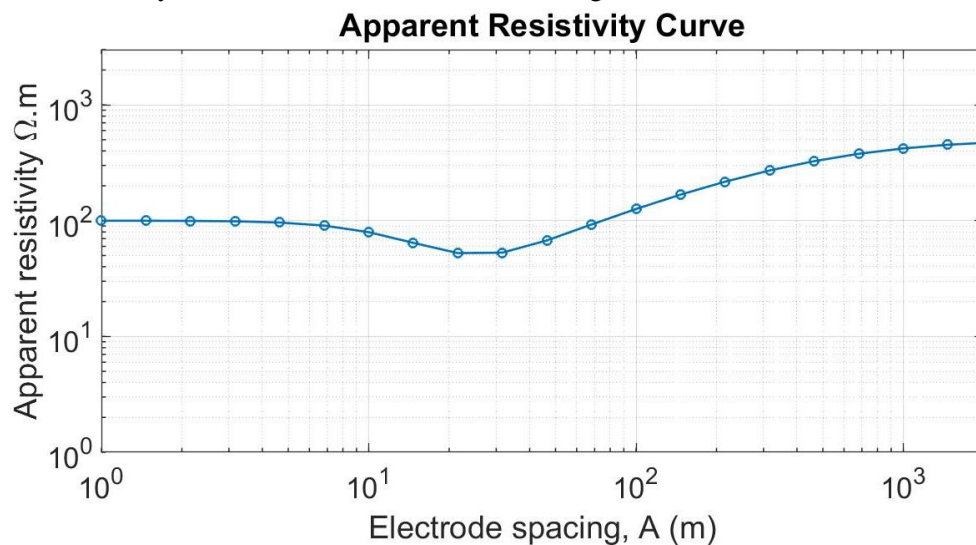
Fig. 5: Apparent resistivity curve for a 3-layer model.

It was noted that the resistivity curve for this model exhibit a minimum which is typical of an H-type model (i.e. $\rho_1 > \rho_2 < \rho_3$). It was observed that the values of electrode spacing (A-value) computed does not fully capture the deeper layer as seen in Fig. 5. The position of the minimum is about two times the depth to the conductor. At small electrode spacing, ρ_a values correspond to the true resistivity of the top layers while at large electrode spacing, ρ_a values correspond to the true resistivity of the bottom layer (Table 1).

Table 1: Computed electrode spacing versus apparent resistivity for the 3-layer model

Electrode Spacing	Apparent Resistivity (Ωm)
1	99.947
1.47	99.855
2.15	99.570

3.16	98.723
4.64	96.379
6.81	90.685
10.00	79.599
14.68	64.332
21.54	52.468
31.62	52.954
46.42	67.545
68.13	92.635
100.00	126.156
146.78	167.926
215.44	217.181
316.23	271.515
464.16	326.821
681.29	378.061
1000.00	420.769

A new resistivity model was generated (Fig. 6) by changing the thickness (H_2) and resistivity (R_2) of the middle layer as thus:

$H_1 = 10$ m, $H'_2 = 30$ m, $R_1 = 100$ Ωm, $R'_2 = 40$ Ωm, $R_3 = 500$ Ωm
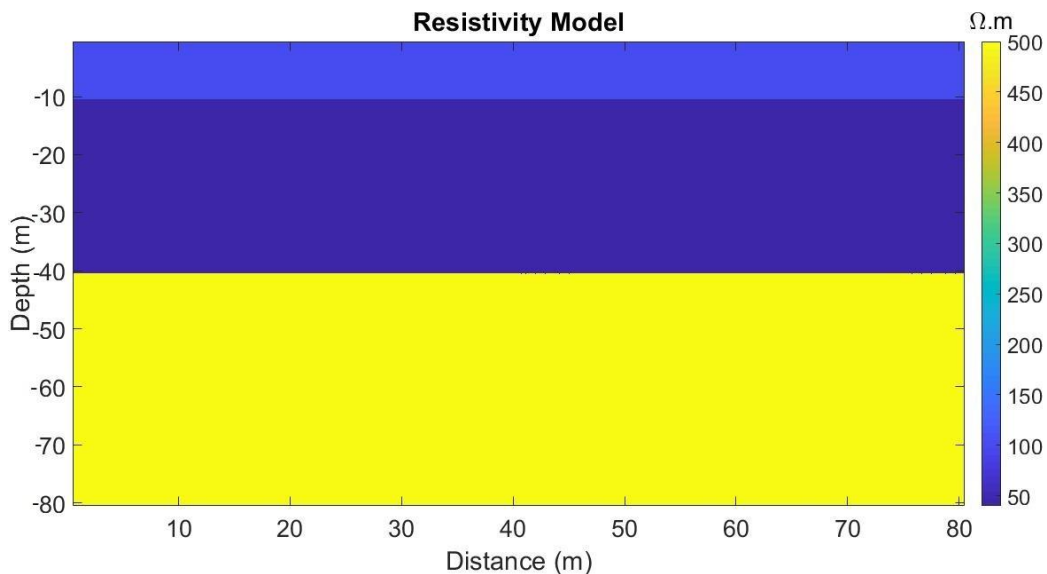
Fig. 6: A new 3-layer resistivity model with different values of thickness and resistivity of intermediate layer.

The apparent resistivity curve is shown in Fig. 7. It was observed that the resistivity curve also exhibit a minimum
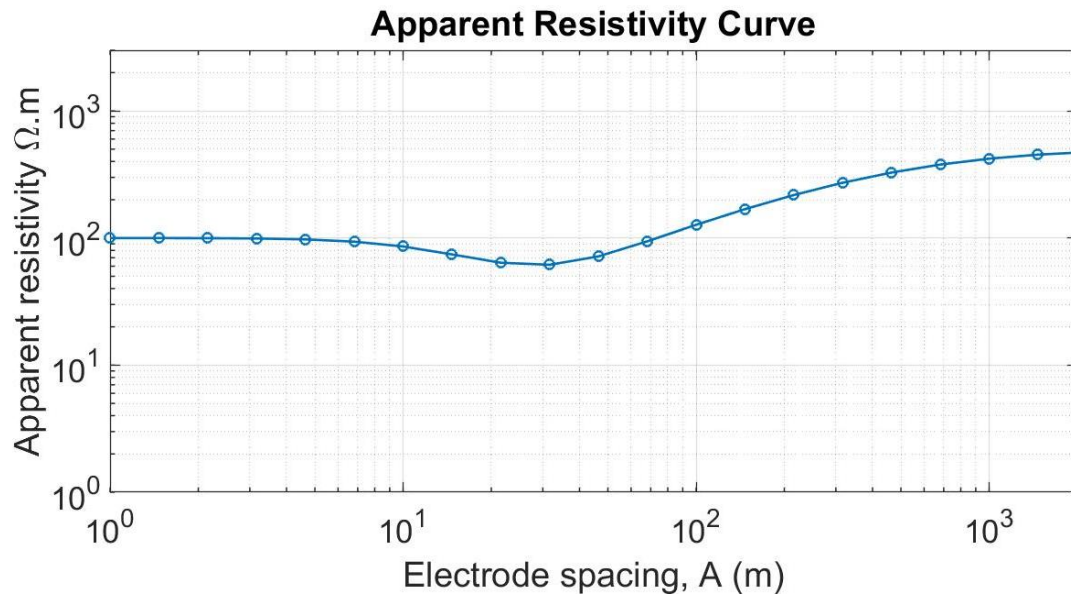
Fig. 7: Apparent resistivity curve for a 3-layer case with different values of thickness and resistivity of middle layer.

Comparing the resistivity curve in Fig. 5 with the curve in Fig. 7, it was observed that despite a different resistivity value of middle layers for the two models, the curves are graphically the same. In these two cases, a conductive layer lies in between two resistive layers, therefore, it might only be possible to estimate the layer conductance, i.e., the thickness divided by the resistivity is constant for the middle layer. Hence a conductive layer and a layer with the double resistivity and double thickness produce equal responses (principle of equivalence leading to ambiguity in 1D geoelectrical interpretation).

However, a new 3-layer model was selected with reduction of thickness of intermediate layer by a factor of 4 as seen in Fig. 8a. It was observed from the resistivity curve in Fig. 8b that as the thickness of the intermediate has decreased by a factor of 4 and keeping all other parameters fixed, the minimum exhibited in the resistivity curve disappears i.e. the middle layer is no longer evident on the apparent resistivity curve and a two-layer case resistivity is observed. This is called the problem of suppression in resistivity sounding i.e. thin layers that have higher resistivity contrast would be detectable, but with equivalence limits resolution of boundary depth.
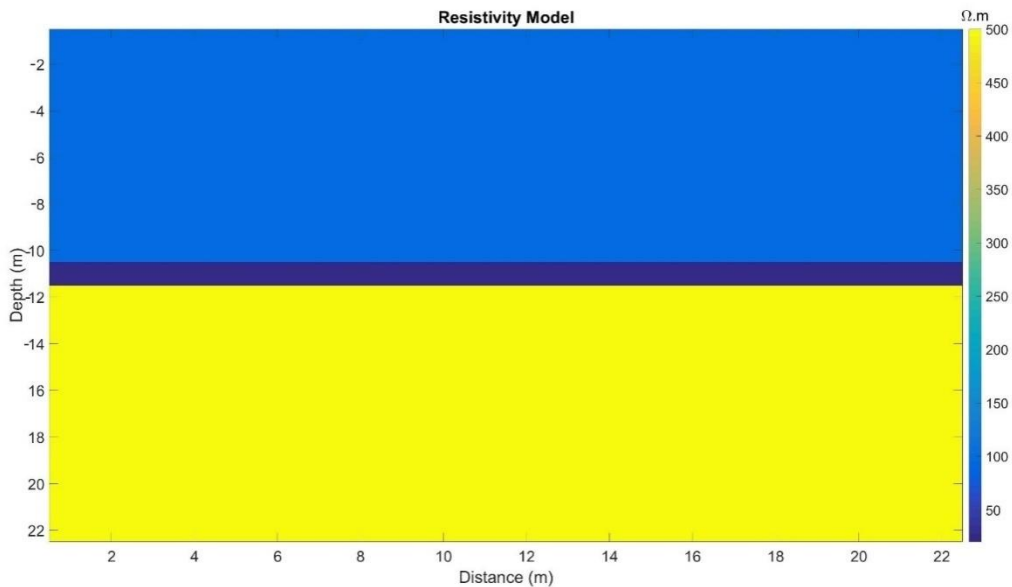
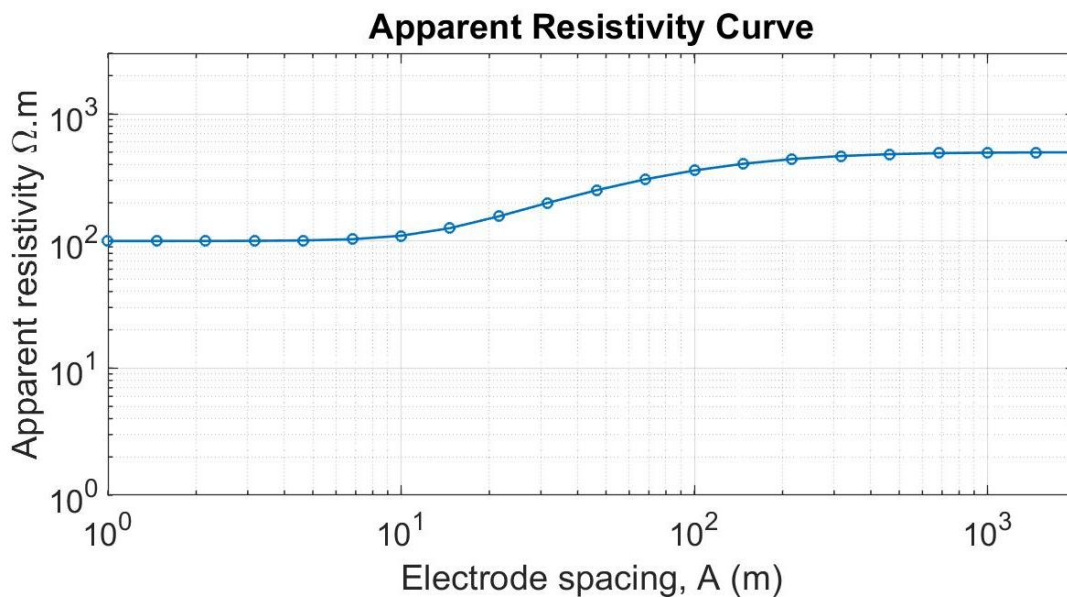Fig. 8a: Resistivity model for a 3-layer case with thin intermediate layer.

Fig. 8b: Apparent resistivity curve for a 3-layer case after reducing the thickness of the intermediate layer by a factor of 4.

Furthermore, the resistivity contrast between the middle layer and the overlying layer was reduced to $R_1 = 100$ Ωm, $R_2 = 80$ Ωm, and it was observed that the principle of suppression still occur i.e. thin layer of small resistivity contrast with respect to background would be omitted (Fig. 9a). Upon reducing the resistivity contrast between the middle layer and the underlying layers, (Fig. 9b) to $R_2 = 400$ Ωm, $R_3 = 500$ Ωm, the problem of suppression still persist, although at different electrode spacing.
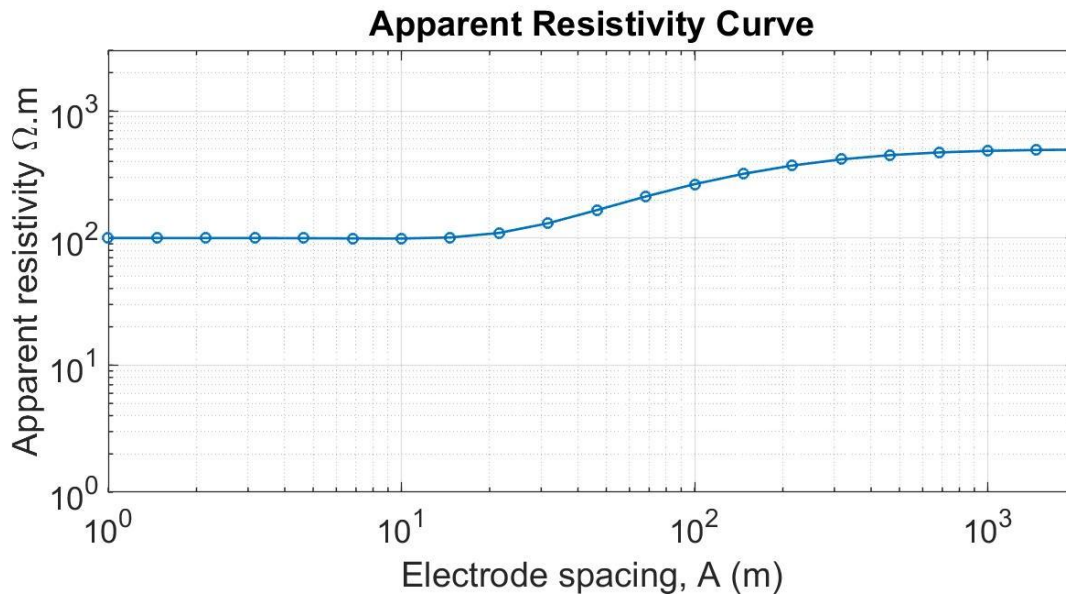
Fig. 9a: Apparent resistivity curve after reducing the resistivity contrast between the intermediate layer and overlying layer
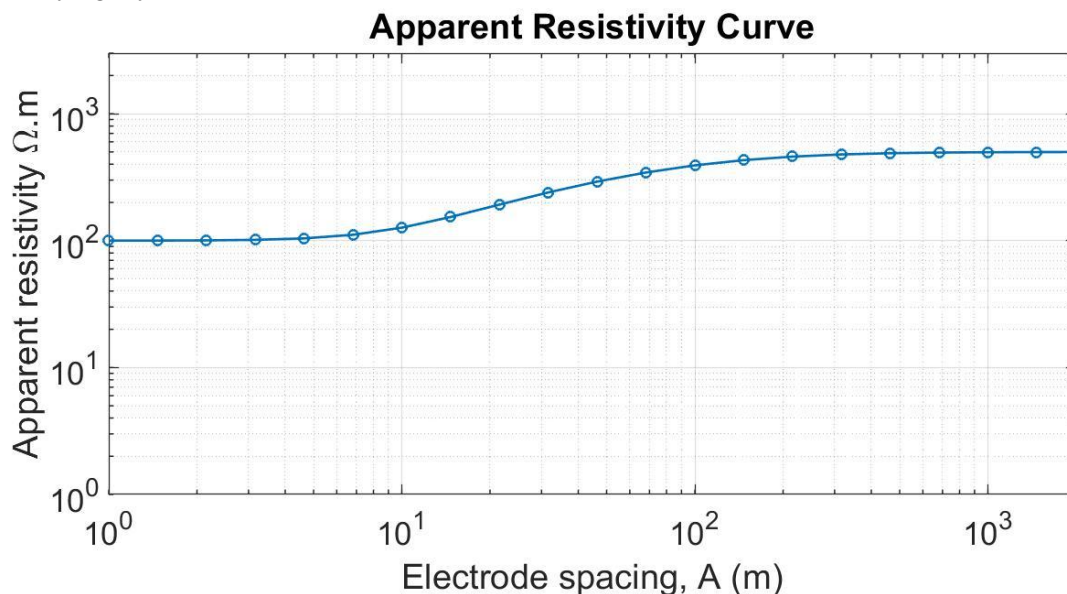

Fig. 9b: Apparent resistivity curve after reducing the resistivity contrast between the intermediate layer and underlying layer.

The implications of the above in practical term are that, a thin freshwater-saturated sandstone overlain by a thick layer of shale and underlain by the basement complex would contribute insignificantly to the resistivity sounding curve; hence, resistivity sounding method would not be able to detect the thin sandstone. Also, any increase in the thickness of the freshwater-saturated sandstone will not be distinguishable from a change in thickness or resistivity of the shale. These problems also occur when using resistivity sounding to detect successive groundwater aquifers [7].

Moreover, a 5-layer model (Fig. 10) was selected and its apparent resistivity curve was plotted. The multilayer model include a target horizon of high resistivity (e.g. a coal layer) in the buried sequence with the following parameters:

$H_1 = 10$ m, $H_2 = 15$ m, $H_3 = 5$ m, $H_4 = 20$ m; $R_1 = 100$ Ωm, $R_2 = 200$ Ωm, $R_3 = 2000$ Ωm, $R_4 = 400$ Ωm, $R_5 = 300$ Ωm.
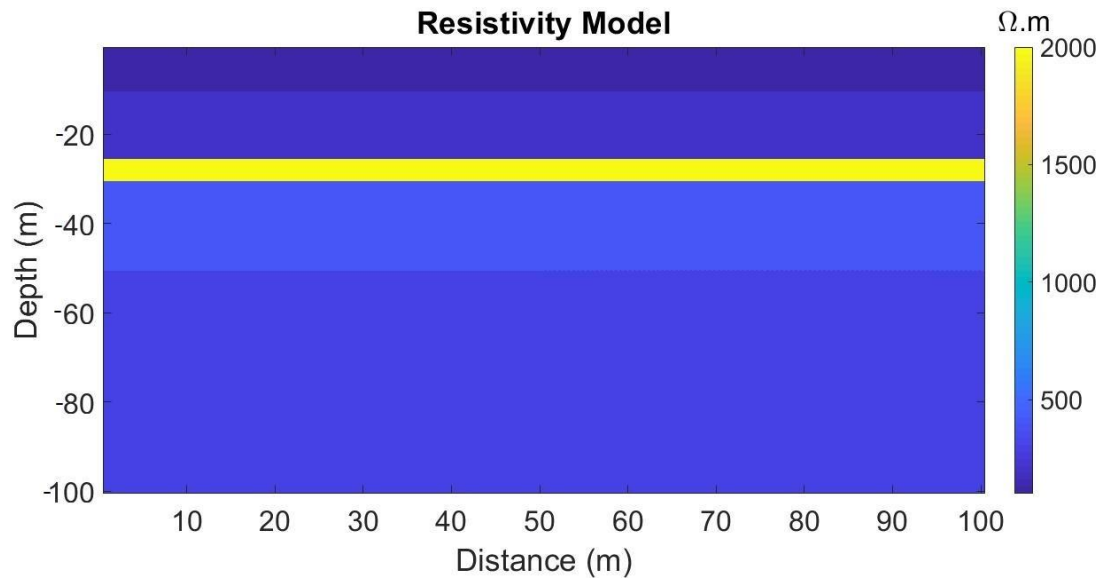
Fig. 10: A 5-layer model. The third layer is highly resistive typical of a coal layer.

The apparent resistivity curve is shown in Fig. 11. It was observed that the high resistivity coal layer is insignificant in the resistivity curve. This means that a thin target (i.e. high resistivity coal seam) at a given depth is not detectable by resistivity sounding. The resistivity of the intermediate layer was put at 2000 Ωm but it is not detectable by sounding (Fig. 11, Table 2).
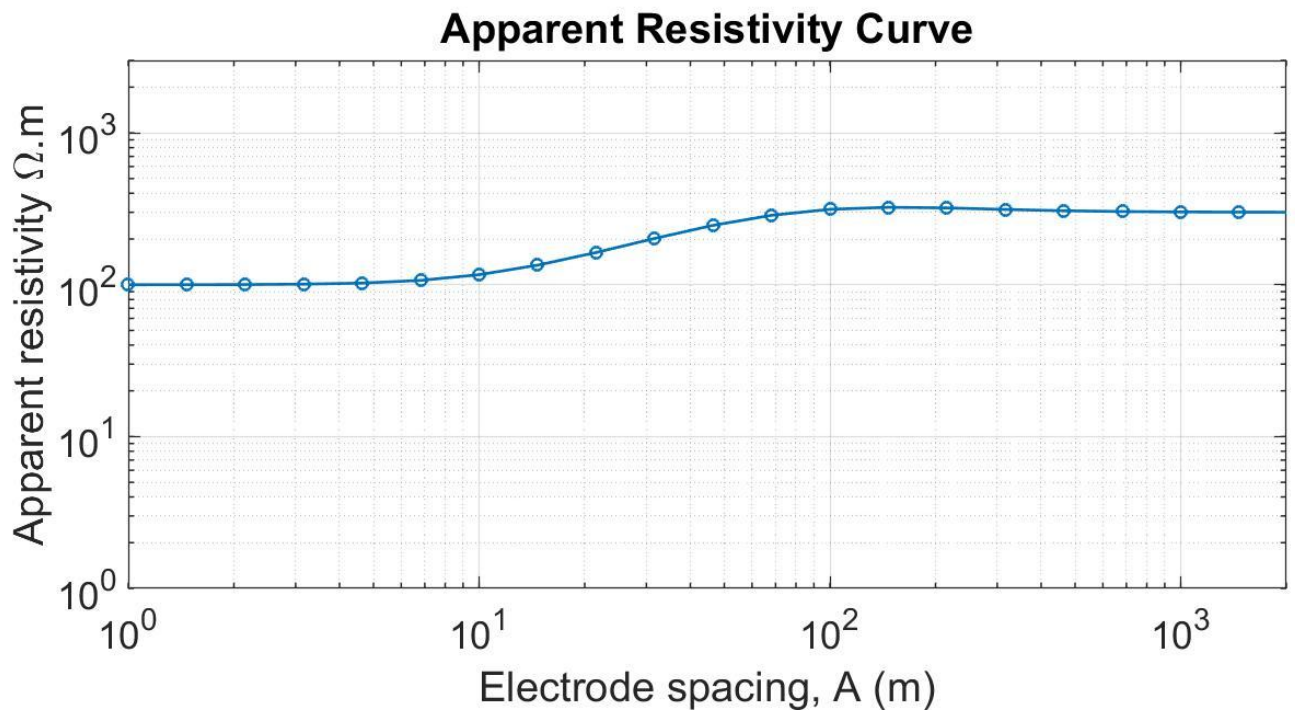

Fig. 11: Apparent resistivity curve for a 5-layer model.

Table 2: Electrode spacing versus apparent resistivity for a 5-layer model

Electrode Spacing	Apparent Resistivity
1.00	100.028
1.47	100.090

2.15	100.283
3.16	100.864
4.64	102.518
6.81	106.807
10.00	116.434
14.68	134.499
21.54	163.006
31.62	201.665
46.42	246.001
68.13	286.592
100.00	313.658
146.78	323.493
215.44	320.548
316.23	313.129
464.16	306.968
681.29	303.375
1000.00	301.581
1467.79	300.731
2154.43	300.333
3162.28	300.147
4641.59	300.063
6812.92	300.026
10000.00	300.011

4. Conclusions

It has been shown from this study that geophysicists should not make any a priori quantitative inferences using the shape of the resistivity sounding curves. This is because two different resistivity models may produce resistivity curves that are essentially the same due to the problems of equivalence and suppression. Understanding these two phenomena would be of use when using resistivity sounding technique for citing boreholes in places underlain by Basement Complex rocks. It would be difficult to identify the fractured/weathered bedrock from the sounding interpretation in such terrain. This is because the resistivity of the weathered layer is usually intermediate between those of the adjacent layers (i.e. residual overburden) on top and the fresh bedrock below. The weathered layer would not be identified on the vertical electrical sounding (VES) curve which may partly be the reason for variations in the depth to bedrock estimated by resistivity sounding interpretation and that confirmed by borehole drilling. To reduce such ambiguity, it is advisable to integrate resistivity sounding data with other geological or geophysical methods to determine the geometries and sizes of features to be investigated or rather combine interpretation of electrical resistivity data with electromagnetic data.

References

[1] Koefoed O(1969)An analysis of equivalence in resistivity sounding. Geophysical Prospecting 17: 327-335.

[2]   Koefoed O (1979) Geosounding principles 1:resistivity sounding measurements, Elsevier, Amsterdam.

[3]   Militzer H, Weber F(1985)AngewandteGeophysik Band 2: Geoelektrik–Geothermik – Radiometrie –Aerogeophysik. Springer Verlag, Wien. 371 pp.

[4]   Telford WM, Geldart LP, Sheriff RE(1990) Applied Geophysics, 2nd ed. Cambridge Univ. Press, Cambridge, 790 pp.

[5]   Simms JE, Morgan FD(1992) Comparison of four least-squares inversion schemes for studying equivalence in one-dimensional resistivity interpretation. Geophysics 57: 1282-1293.

[6]   Zohdy AA (1974) Application of surface geophysics to groundwater investigation techniques of water resources investigations of the US Geological Survey, Book 2, pp. 5-66.

[7]   Olayinka AI(1997)Error in depth determination from resistivity soundings due to non-identification of suppressed layers. Journal of African Earth Sciences 24(4): 635-647.

[8]   Hoffmann R, Dietrich P(2004)An approach to determine equivalent solutions to the geoelectrical 2D inversion problem. Journal of Applied Geophysics 56: 79– 91.

[9]   Batayneh AT, Al-Zoubi AS, Abu-Ajamieh MM(2004)Geoelectrical soundings and their relationship to channel seepage areas at the Kaffrein Dam, Jordan. Journal of Applied Sciences 4 (1): 28-37.

[10]   Niwas S, de Lima (2006)Unified equation for straightforward inversion scheme on vertical electrical sounding data. Geofizika 23(1): 21-35.

[11]   Ojo AO, Olorunfemi MO(2013)A graphical and semi-quantitative technique for investigating vertical electrical sounding (VES) curves for indices of confined fractured basement column. The Pacific Journal of Science and Technology 14(2): 537-550.

[12]   Kunetz G (1966) Processing and interpretation of magnetotelluric soundings. Geophysics 37: 1000-1021.

[13]   Biswas A, Mandal A, Sharma SP, Mohanty WK. (2014) Integrating apparent conductance in resistivity sounding to constrain 2D gravity modeling for subsurface structure associated with uranium mineralization across south purulia shear zone, west Bengal, India. International Journal of Geophysics 2014, Article ID 691521, 8 pages http://dx.doi.org/10.1155/2014/691521.

[14]   Carruthers RM, Smith IF(1992)The use of ground electrical survey methods for siting water-supply boreholes in shallow crystalline basement terrains. In: Hydrogeology of Crystalline Basement Aquifers in Africa (Edited by Wright, E. P. and Burgess, W. G.) Geological Society Special Publication 66, 203-220.

[15]   Hazell JRT, Cratchley CR. Jones, CRC(1992)The hydrogeology of crystalline aquifers in northern Nigeria and geophysical techniques used in their exploration. In: Hydrogeology of Crystalline Basement Aquifers in Africa (Edited by Wright, E. P).

[16]   Olorunfemi MO, Olorunniwo MA(1985)Geoelectric parameters and aquifer characteristics of some parts of southwest Nigeria. GeologiaApplicataIdrogeologia 20: 99-109.

[17]   Ghosh DP (1971) Inverse filter coefficients for the computation of the apparent resistivity standard curves for horizontally stratified earth.Geophysical Prospecting19:769–775.

[18]   Davis PA, Greenhalgh S, Merrick N(1980) Resistivity sounding computation with any array using a single digital filter. Bulletin of Australian Society of Exploration Geophysics 11(½): 54-62.

[19]   Mooney HM, Orellana E, Pickett H, Tornheim L (1966) A resistivity computation method for layered earth model, Geophysics31:192–203.